

# Effect of Oxygen Addition on Polycyclic Aromatic Hydrocarbon Formation in 1,3 Butadiene Counter-Flow Diffusion Flames

NESRIN OLTEN and SELIM SENKAN\*

*Department of Chemical Engineering, University of California, Los Angeles, Los Angeles, CA 90095, USA*

The effect of 3% O<sub>2</sub> addition to the fuel on detailed chemical structure of a 1,3 butadiene counter-flow diffusion flame has been investigated by using heated microprobe sampling and online gas chromatography mass spectrometry. Centerline gas temperature and species mole-fraction profiles were measured both in the absence and presence of oxygen on the fuel side. The rapid thermocouple insertion method was used to obtain the flame temperature profiles. Although the addition of oxygen to the fuel side did not significantly change the shape and peak values of the temperature profiles, species mole-fraction profiles were significantly altered. Flame reactions started earlier in the presence of oxygen in the fuel, resulting in the shift of the reaction zone toward the fuel burner port. The presence of oxygen in the fuel led to decreased peak mole fractions of the aromatic and two-ring polycyclic aromatic hydrocarbon species. In contrast, the peak mole fractions of polycyclic aromatic hydrocarbon having three or more rings significantly increased in the presence of oxygen in the fuel stream. An analysis of the data suggests the need to invoke new reaction mechanisms describing the formation and destruction of polycyclic aromatic hydrocarbon. © 2001 by The Combustion Institute

## INTRODUCTION

The emission standards of combustion have been steadily reduced in recent years, and a large research effort has been focused on lowering the emission of nitrogen oxides, hydrocarbon, and particulate matter. Addition of oxygenates to fuel reduces these pollutants by reducing the flame temperatures and by altering the combustion chemistry [1]. Oxygenate addition also reduces the level of precursors, specifically acetylene, 1, 3 butadiene, propargyl, and vinyl radicals in combustion process, which are responsible for the formation of aromatic and polycyclic aromatic hydrocarbon (PAH) species and soot in flames [2]. Consequently, the development of a better understanding of its combustion chemistry is of practical and scientific interest. Previously, the combustion of 1,3 butadiene has been studied with regard to soot formation in co-flowing diffusion flames [3–6]. In some of these studies, it was advocated that flame temperature should be the controlling parameter for soot formation due to its direct impact on fuel pyrolysis, thus soot nucleation, rates [5]. The addition of oxygen to the fuel side also increased soot formation, and this was also

attributed to increased stoichiometric flame temperature [6].

PAH formation in low-pressure premixed flames of 1,3 butadiene were also studied by using molecular beam sampling mass spectrometry [7]. These investigators reported the species mole-fraction profiles up to two-ring PAH, and provided kinetic arguments on PAH and soot formation based on species flux analysis. Most recently, stack emissions of PAH from vapor and pool fires of 1,3 butadiene were determined using sorbent adsorption followed by gas chromatography mass spectrometry [8]. Accordingly, sooting tendency was found to increase with increasing equivalence ratio and decreased with increasing temperature. The kinetics of the elementary reactions of 1,3 butadiene were also studied [9–14].

However, despite the significance of 1,3 butadiene in PAH and soot formation processes in hydrocarbon combustion, we are not aware of any studies in which the detailed chemical structures of the flames of 1,3 butadiene have been reported. In this paper, we focused on the effect of oxygen on PAH formation and reported detailed structure of opposed jet diffusion flames of 1,3 butadiene both in the absence and presence of oxygen added to the fuel side. Related research is also in progress in premixed flames, and will be reported later.

\*Corresponding author. E-mail: senkan@ucla.edu

TABLE 1  
1,3 Butadiene Flame Conditions

Pure butadiene flame		Oxygen-added butadiene flame	
Fuel side		Fuel side	
C <sub>4</sub> H <sub>6</sub> mole fraction	0.50	C <sub>4</sub> H <sub>6</sub> mole fraction	0.50
Ar mole fraction	0.50	Ar mole fraction	0.47
Oxygen mole fraction	0.00	Oxygen mole fraction	0.03
Gas velocity, $v_f$ , cm/s	13.16	Gas velocity, $V_f$ , cm/s	13.16
Fuel side density, $\rho_f$ , g/L	1.92	Fuel side density, $\rho_f$ , g/L	1.87
Oxidizer side		Oxidizer side	
Oxygen mole fraction	0.22	Oxygen mole fraction	0.22
Ar mole fraction	0.78	Ar mole fraction	0.78
Gas velocity, $V_o$ , cm/s	16.12	Gas velocity, $V_o$ , cm/s	16.12
Burner separation, L, cm	1.65	Burner separation, L, cm	1.64
Strain rate <sup>a</sup> , K, s <sup>-1</sup>	37.6	Strain rate <sup>a</sup> , K, s <sup>-1</sup>	37.6

<sup>a</sup> Strain rate was calculated by using the equation:  $K = (2V_o/L)\{1 + (V_f/V_o)(\rho_f/\rho_o)^{0.5}\}$ , [s<sup>-1</sup>].

## EXPERIMENTAL METHOD

Details of the counter-flow diffusion burner system that has been used in the experiments and the method of quantification in obtaining the species mole-fraction profiles can be found in our previous paper [15], thus will not be repeated. Flame samples were withdrawn by using a heated (300°C) quartz microprobe (0.635-cm outer diameter) with a  $200 \times 10^{-4}$  cm diameter orifice at its tapered tip. The probe orifice diameter used was the smallest possible size to achieve sampling in such sooting flames. Soot particles in the sample were trapped by using a heated quartz filter before gas analysis. As discussed earlier, the system developed allows the quantitative determination of mole-fraction profiles for PAH up to five rings (252 Daltons) [15]. The accuracies for the determination of species mole fraction were estimated to be ~15%.

Gas temperature measurements were accomplished by using a silica coated Pt/Pt + 13%Rh (R type, Omega) thermocouple with 0.075 mm wire and a bead diameter of 0.200 mm. Rapid insertion technique was applied in order to obtain the profiles. A data acquisition board (5580Sci, American Data Acquisition Corporation, Los Angeles, CA) was used to digitize analog inputs for computer data collection. Stepper motors and the data-acquisition board were controlled via LABVIEW. In this method, the thermocouple was quickly introduced into

the flame by using a computer-controlled driver mechanism, and the data acquired automatically after insertion. In order to minimize heat conduction along the wires, the thermocouple was positioned parallel to the burner surface. In the sooting parts of the flame, the soot deposits were burnt off with a propane torch between each measurement. After soot burn off, the thermocouple was also inspected by a microscope to insure that its surface was clean and ready for the next insertion. Here we report the peak thermocouple readings without any radiation corrections.

## RESULTS AND DISCUSSION

Two flames of 1,3 butadiene were studied, and the experimental conditions used are given in Table 1. These conditions were selected after considering a number of different conditions to determine the most suitable sets for flame sampling and temperature measurement. As seen from Table 1, the two flames studied essentially were the same with the exception of 3% O<sub>2</sub> that was introduced into the fuel side of the second flame.

In order to obtain accurate temperature profiles, it is necessary to consider thermocouple disturbances and radiation effects. Unfortunately, in fuel-rich flames, soot accumulation on the thermocouple significantly complicates the latter, rendering the acquisition of reliable tem-

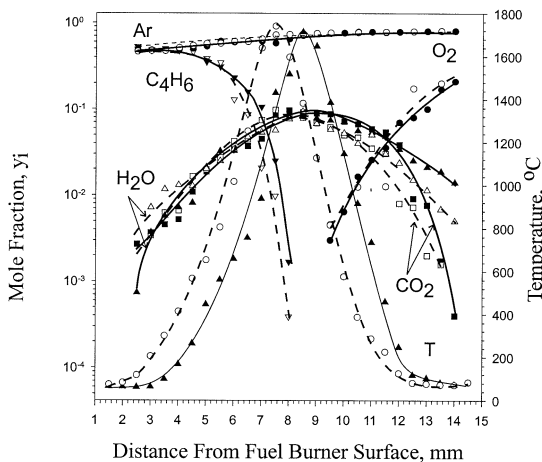


Fig. 1. Major species and temperature profiles for both pure butadiene and oxygen-doped butadiene flame. In this figure and all the following, symbols are experimental data points (filled symbols butadiene, and empty symbols oxygen-doped butadiene flames), and lines show the trend lines.

perature measurements very difficult. With the implementation of the rapid insertion method and computerized data acquisition, we believe we generated a practical optimum set of conditions for temperature measurement. The temperature profiles shown in Fig. 1 show that the maximum centerline flame temperatures measured at 8.5 mm for the pure butadiene flame and at 7.5 mm for the  $O_2$  added butadiene flame, respectively. In Fig. 1, as well as in subsequent figures, the symbols represent the experimental data (hollow symbols for the oxygen-doped fuel flame), whereas the lines indicate trends. As seen in Fig. 1, for the pure butadiene flame, the maximum temperature reached was 1713°C, which is well below the stoichiometric flame temperature (2000°C) of butadiene in air [16]. The difference is most likely due to radiation losses from the thermocouple and the flame. Another reason may be that, a diffusion flame may not reach stoichiometric flame temperatures due to incomplete conversion of CO to  $CO_2$  (nonequilibrium effects) [17]. It is interesting to note that the oxygenated butadiene flame exhibited only a slightly higher peak temperature of 1740°C.

Within spatial resolution of the thermocouple measurements, the maximum flame temperature, which correspond to the main reaction zone, is generally situated at the same position

as the visible blue-flame surface. As it can be expected, the addition of  $O_2$  into the fuel stream caused a change in temperature distribution inside the flame. Neglecting the temperature change along radial direction within the flame, we can use the centerline temperature measurements of the flames to make a comparison. The data lead to the conclusion that, addition of  $O_2$  into fuel stream causes only minor changes in the maximum flame temperature (27°C). The major impact of oxygen addition appears to be to lower the position of the flame front toward the fuel burner surface. This results in the earlier pyrolysis of the fuel in the presence of  $O_2$  causing a shift in the position of the flame front.

Additives can effect the behavior of diffusion flames in several ways. They can undergo chemical reactions with the fuel or fuel pyrolysis products and initiate the combustion process earlier. The additives can also act as a participating species in heat transfer by altering the mixture thermal diffusivity, or they can serve as a heat sink via their heat capacity [4]. As can be seen in Fig. 1, the temperature increases earlier in the  $O_2$  added flame. Because the maximum flame temperatures were very close to one another, and fact that the molecular diffusivity of oxygen is only slightly larger than butadiene, the primary effect of added  $O_2$  to the fuel side appears to be chemical in nature. This is also supported by the rapid decrease in the fuel mole fraction and the earlier formation of  $H_2O$  (Fig. 1). In fact, it is well known from fuel pyrolysis experiments that the addition of small amount of oxygen can accelerate the pyrolysis process [18]. Therefore, it is not surprising to see a more rapid decline in the fuel profile in the fuel-rich side of the flame in the present experiments.

In Figs. 2 and 3 the mole-fraction profiles for  $H_2$ , CO,  $CH_4$ ,  $C_2H_6$ ,  $C_2H_4$ ,  $C_2H_2$ , and  $C_3H_4$  are presented, in which the latter two are believed to be important PAH precursors [19–21]. As seen in these figures, the peak  $C_3H_4$  mole fractions decreased by the addition of  $O_2$  to the fuel side in the order of 4%, where the peak  $C_2H_2$  mole fraction decreased 11%. Although these changes are within the limits of accuracy of our measurements, systematic variations were clear, especially when the data are plotted on a linear basis. Consistent with earlier pyrolysis, hydrogen levels in the oxygenated buta-

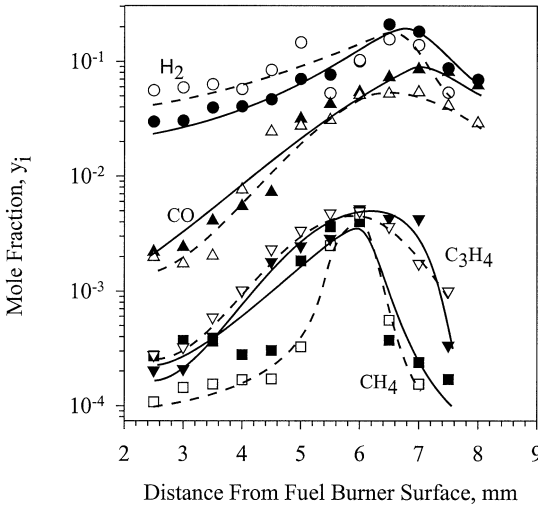


Fig. 2. CO, H<sub>2</sub>, CH<sub>4</sub>, and C<sub>3</sub>H<sub>4</sub> mole-fraction profiles.

diene flame were higher. Another interesting observation is the reduction of the CO/CO<sub>2</sub> ratio from 0.88 in the 1,3 butadiene flame to 0.55 in the oxygen-doped flame.

In Fig. 4, the mole-fraction profiles of C<sub>4</sub> products are presented. As seen in this figure, vinylacetylene and diacetylene maximum mole fractions did not change much by the addition of O<sub>2</sub> to the fuel side. However, significant differences were present closer to the fuel burner surface, in accordance with the earlier start on the pyrolysis reactions in the presence of oxygen. Butadiene is proposed to be the precursor

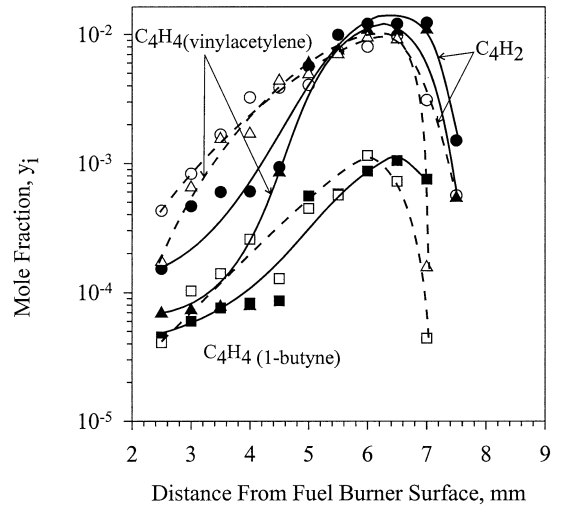


Fig. 4. Carbon containing aliphatic pyrolysis product mole-fraction profiles.

to vinylacetylene formation, whereas vinylacetylene is precursor to diacetylene formation [20]. Another way of forming diacetylene was proposed by Miller and Melius, involving the reaction between acetylene and C<sub>2</sub>H. This mechanism implies that the decreasing C<sub>2</sub>H<sub>2</sub> levels should also decrease the diacetylene level, which is consistent with our experiments [22].

The mole-fraction profiles for C<sub>5</sub> products are presented in Fig. 5. In this figure, it is seen that cyclopentadiene levels are higher in the oxygen-doped flame than pure butadiene flame

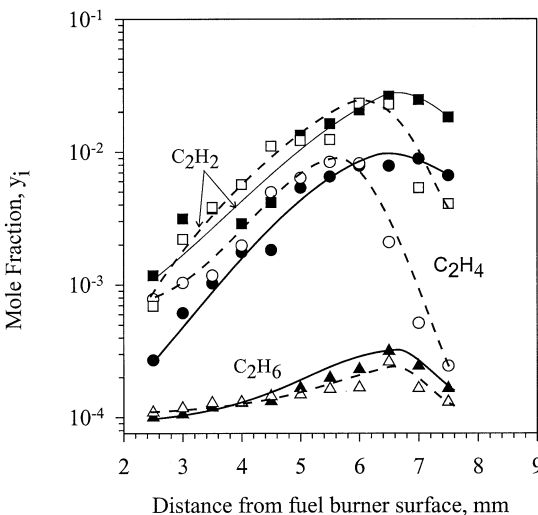


Fig. 3. Carbon containing aliphatic pyrolysis product mole-fraction profiles.

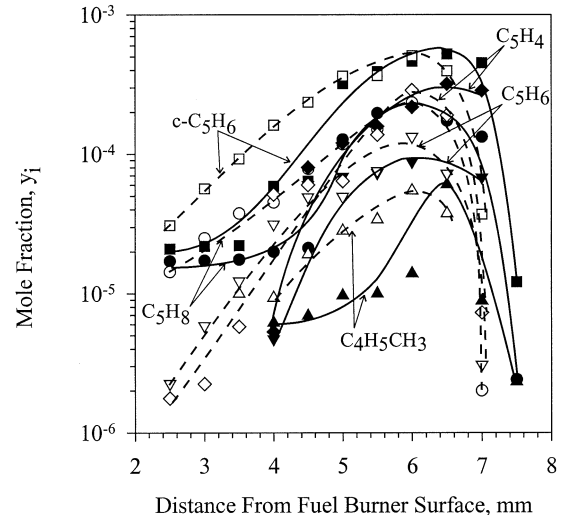


Fig. 5. Carbon containing aliphatic pyrolysis product mole-fraction profiles.

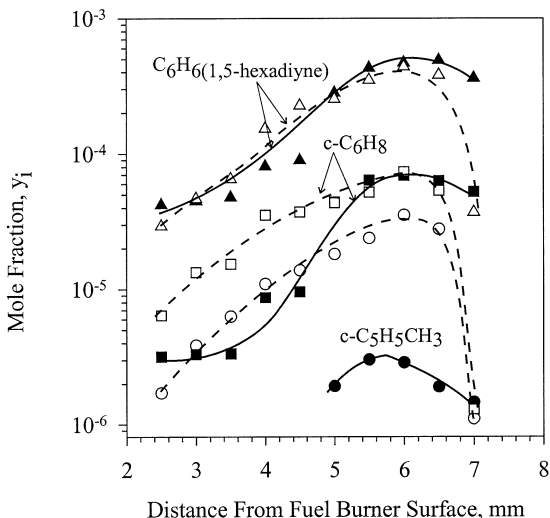


Fig. 6. Carbon containing aliphatic pyrolysis product mole-fraction profiles.

over the entire fuel-rich zone, i.e., until the peak is reached. As noted earlier, the general behavior of the oxygen-doped flame is the early formation of pyrolysis and oxidative pyrolysis products. The results presented in Fig. 5 are consistent with this picture.

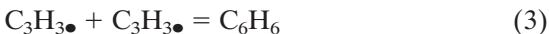
Recent attempts to understand the detailed kinetic mechanism of PAH formation in flames relied on the use of data ethylene, acetylene, or small alkane flames [19–23]. These investigations let to the following reaction as the dominant route for benzene formation:



as well as the reaction of the *n*-C<sub>4</sub>H<sub>3</sub> radical with acetylene to form phenyl radical,



Alternately, benzene formation was also suggested to proceed via the recombination of the resonance stabilized propargyl radicals [24,25]:



If any of these reactions were to dominate benzene formation process, one would expect a decrease in benzene levels on the oxygenated butadiene flame because the peak mole fractions of both the acetylene and C<sub>3</sub>H<sub>4</sub> decreased relative to the pure butadiene flame. The 15%

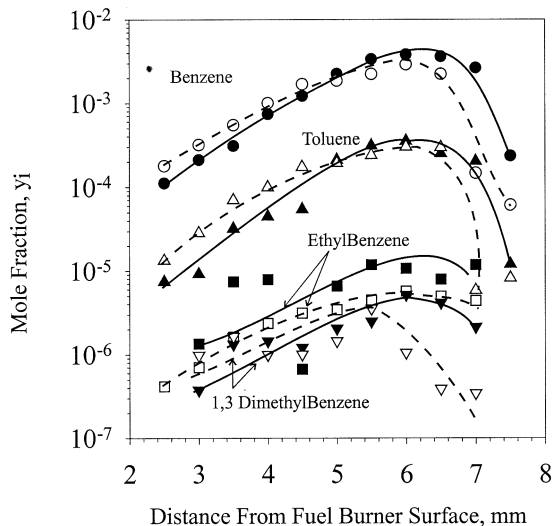


Fig. 7. Benzene and alkyl group substituted one-ring aromatic species mole-fraction profiles.

decrease in the peak benzene level is closer in magnitude to the decrease in C<sub>2</sub>H<sub>2</sub> levels in the oxygen-doped flame, suggesting that the majority of benzene formation should be via reactions [1] and [2] [19].

The effect of oxygen presence in the fuel side had a similar impact on the higher aromatic hydrocarbon products as shown in Figs. 8 and 9. The maximum level of phenyl acetylene and styrene mole fractions also decreased 15%, similar to benzene. The growth from benzene to larger aromatics has been attributed to succes-

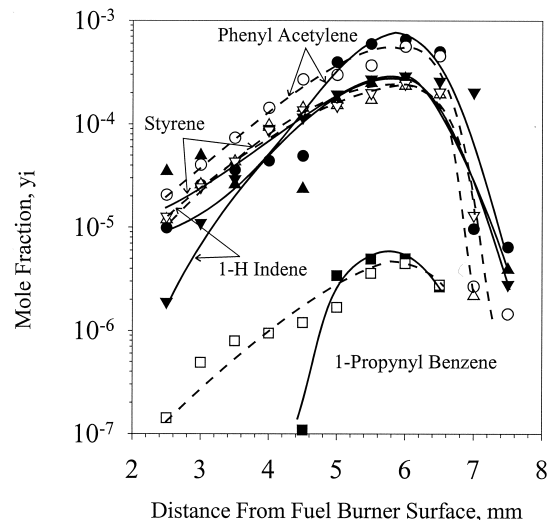


Fig. 8. Ring aromatic species mole-fraction profiles.

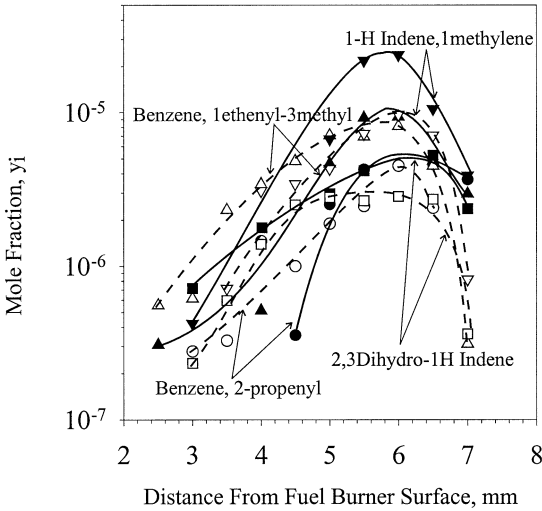


Fig. 9. Ring aromatic species mole-fraction profiles.

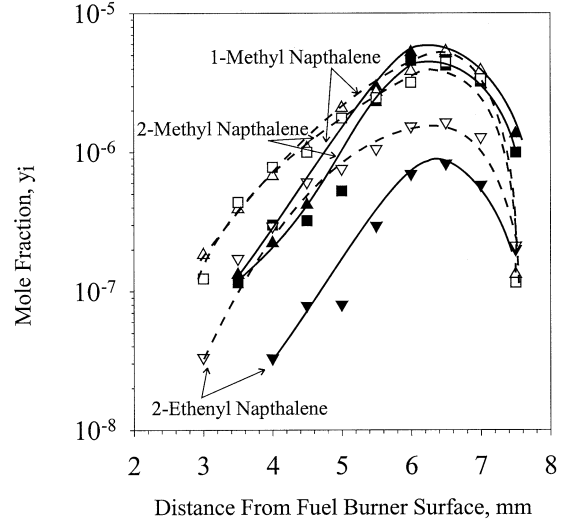


Fig. 11. Ring aromatic species mole-fraction profiles.

sive addition of  $C_2H_2$  [26]. This mechanism implies that the effect of oxygen doping on larger aromatics should be similar to those on benzene, a result consistent with our measurements.

These trends were also observed for the mole-fraction profiles of two-ring polycyclic aromatic hydrocarbons presented in Figs. 10, 11, and 12. Naphthalene formation is the first step in the growth process to larger PAH molecules. The decrease in the maximum level of naphthalene was about 20% in the case of oxygen added flame. This suggests that another mechanism, other than  $C_2H_2$  addition, must also be opera-

tive under the experimental conditions. Indeed, such an alternative pathway, involving the reaction of two cyclopentadienyl radicals has been suggested [27]. However, because the cyclopentadiene maximum levels were nearly the same in both flames, the decrease in naphthalene level in the oxygenated butadiene cannot be explained by this mechanism either. It appears that naphthalene undergoes subsequent reactions in the presence of oxygen. This is supported by the presence of a large number of products containing the naphthalene backbone (Figs. 10 and 11).

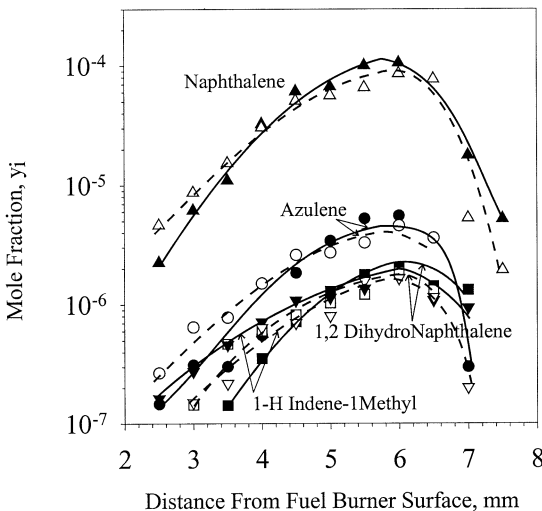


Fig. 10. Ring aromatic species mole-fraction profiles.

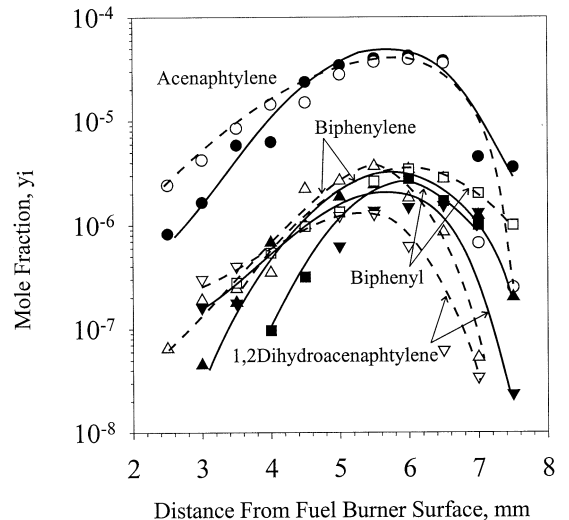


Fig. 12. Ring aromatic species mole-fraction profiles.

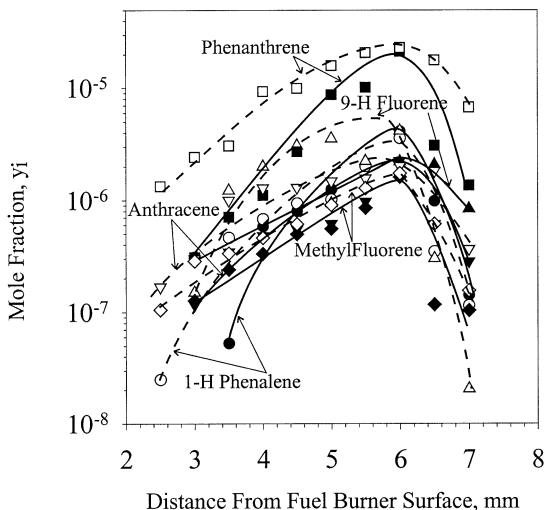


Fig. 13. Ring aromatic species mole-fraction profiles.

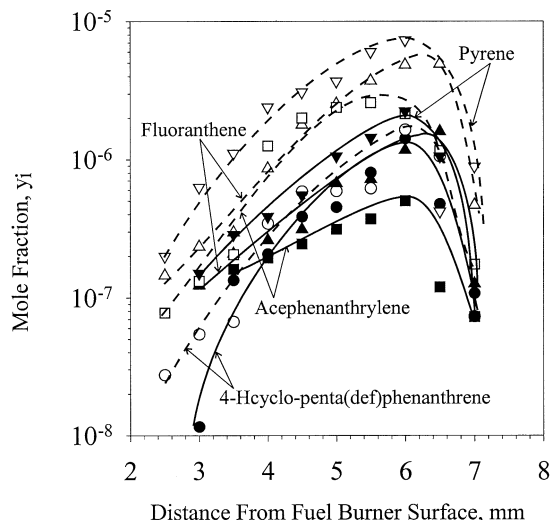


Fig. 14. Ring aromatic species mole-fraction profiles.

PAH with five-membered rings are believed to have important role in molecular weight growth processes in the gas phase because of the reactivity of the double bond [28]. Acenaphthylene, which can be produced by the addition of acetylene to naphthalene, was also detected in both flames and as in the case with other hydrocarbons, its peak level was lower in the presence of added oxygen (Fig. 12). On the other hand, the drop in acenaphthylene was not as large as drop in  $C_2H_2$  level, which again suggests that  $C_2H_2$  addition is not the only route in PAH growth process.

The mole-fraction profiles of PAH possessing three and four aromatic rings are presented in Figs. 13 and 14. It is interesting to note that species with three or more rings were more abundant in the oxygen-doped flame than the pure butadiene flame. Evidently, oxygen addition promotes the formation of higher molecular weight PAH, and not the smaller aromatics. Phenanthrene is another key species for PAH growth and has been suggested to form by the sequential addition of  $C_2H_2$  to naphthalene [19], and the reaction of  $C_2H_2$  with biphenyl radicals [29]. Phenanthrene mole fractions reached about 20 ppm and 15 ppm in the oxygen-doped and the pure butadiene flame, respectively. As shown earlier in Fig. 10, naphthalene levels were lower in the oxygenated butadiene flames. This combined with lower  $C_2H_2$  levels cannot account for the increased

phenanthrene levels in the oxygen-doped flame. Alternately, although the peak biphenyl levels were  $\sim 20\%$  higher in the oxygenated butadiene flame, at 3.5 ppm it cannot account for the formation of 20 ppm phenanthrene. These results clearly suggest that other pathways for the formation of larger PAH must be put forward to account for the experimental results.

The PAH growth progressed further in the case of oxygen-doped flame, forming cyclopenta(cd)pyrene and its isomer benzo(ghi)fluoranthene as the largest detectable PAH (Fig. 15). These PAH were not detected in the pure butadiene flame. As noted earlier, some oxygenated aromatic species, such as furan, benzaldehyde, and phenol, were also produced in the oxygen-doped flame and these are presented in Fig. 15. With the exception of furan, all the other oxygenates reached their peak levels before the PAH. For the case of furan, its mole-fraction profile exhibited its maximum later, at about the same flame height as the PAH.

## CONCLUSIONS

In summary, although the addition of oxygen to the fuel side of a 1,3 butadiene counter-flow diffusion flame did not significantly change the shape and peak values of the temperature profile, species mole-fraction profiles were significantly altered. Flame reactions started earlier in

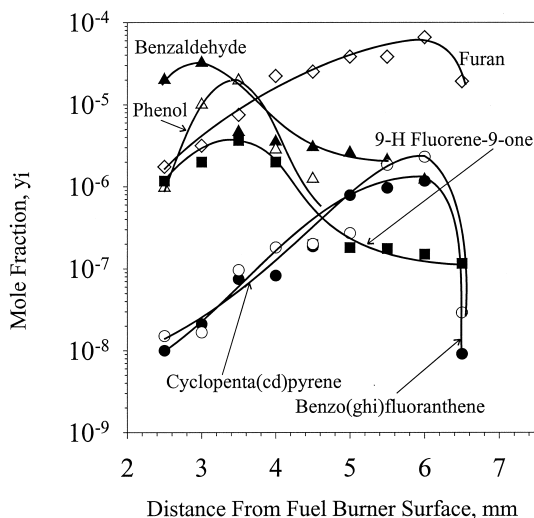


Fig. 15. Cyclopenta(cd)pyrene, benzo(ghi)fluoranthene, and oxygenated species mole-fraction profiles formed only in the oxygen-doped butadiene flame.

the presence of oxygen in the fuel, resulting in the shift of the reaction zone toward the fuel burner port. The presence of oxygen in the fuel led to decreased peak mole fractions of the aromatic and two-ring PAH species. In contrast, the peak mole fractions of PAH having three or more rings significantly increased in the presence of oxygen in the fuel stream. Analysis of the data suggests the need to invoke new reaction mechanisms describing the formation and destruction of PAH.

*This work was supported, in part, by the National Science Foundation and the U.S. Environmental Protection Agency. The authors also thank Kitty Lee and Manabu Yamamoto for their help with the experiments.*

## REFERENCES

1. Curran, H. J., Glaude, P. A., Marinov, N. M., Pitz, W. J., and Westbrook, C. K., *Fall Meeting of the Western States Section of the Combustion Institute*, October 25–26, 1999.
2. Flynn, P. F., Durrett, R. P., Hunter, G. L., zur Loye, A. O., Akinoyemi, O. C., Dec, J. E., and Westbrook, C. K., Society Of Automotive Engineers Publication SAE-01-0509, 1999.
3. Wegert, R., Wiese, W., and Homann, K. H., *Combust. Flame* 95:61–75 (1993).
4. Schug, K. P., Manheimer-Timnat, Y., Yaccarino, P.,

- and Glassman, I., *Combust. Sci. Tech.* 22:235–250 (1980).
5. Gomez, A., Sidebotham, G., and Glassman, I., *Combust. Flame* 58:45–57 (1984).
6. Glassman, I., and Yaccarino, P., *Combust. Flame* 24: 107–114 (1980).
7. Cole, J. A. (1982). M. S. Thesis, Department of Chemical Engineering, Massachusetts Institute of Technology, Cambridge, MA.
8. Catalo, W. J., *Chemosphere*, 143–147 (1998).
9. Benson, S., *J. Chem. Physics* 46:4920–4926 (1967).
10. Harkness, J. B., Kistiakowsky, G. B., and Mears, W. H., *J. Chem. Physics* 5:682–694 (1937).
11. Kistiakowsky, G. B., and Ransom, W. W., *J. Chem. Physics* 7:725–735 (1939).
12. Benson, S. W., and Haugen, G. R., *J. Phys. Chem.* 71:1735–1746 (1967).
13. Brezinsky, K., Burke, E. J., and Glassman, I., *Twentieth International Symposium on Combustion*, The Combustion Institute, Pittsburg, 1984, pp. 613–622.
14. Dagaut, P., and Cathonnet, M., *Combust. Flame* 113: 620, 1998.
15. Olten, N., and Senkan, S. M., *Combust. Flame* 118: 500–507 (1999).
16. Glassman, I., *Combustion* (2nd ed.) Academic Press, San Diego, 1997, p. 23.
17. Macek, A., *Flammability Limits: Thermodynamics And Kinetics*, National Bureau of Standards Internal Report 76-1076 (1976).
18. Smith, S. R., and Gordon, A. S., *J. Phys. Chem.* 60:759 (1956).
19. Frencklach, M., and Warnatz, J., *Combust. Sci. Tech.* 51:265–283 (1987).
20. Markatau, P., Wang, H., and Frencklach, M., *Combust. Flame* 93:467–482 (1993).
21. Kazakov, A., Wang, H., and Frencklach, M., *Combust. Flame* 100:111–120 (1995).
22. Miller, J. A., and Melius, C. F., *Combust. Flame* 91:21–39 (1992).
23. Seshadri, K., Mauss, F., Peters, N., and Warnatz, J., *Twenty-Third International Symposium On Combustion*, The Combustion Institute, Pittsburg, 1990, pp. 559–566.
24. Marinov, N. M., Pitz, W. J., Westbrook, C. K., Castaldi, M. J., and Senkan, S. M., *Combust. Sci. Tech.* 116–117:211–287 (1996).
25. Leung, K. M., and Lindstedt, R. P., *Combust. Flame* 102:129–160 (1995).
26. Wang, H., and Frencklach, M., *Combust. Flame* 110: 173–221 (1997).
27. Dean, A. M., *J. Phys. Chem.* 94:1432 (1990).
28. Benish, T. G., Lafleur, A. L., Taghizadeh, K., and Howard, J. B., *Twenty-Sixth International Symposium On Combustion*, The Combustion Institute, Pittsburg, 1996, pp. 2319–2326.
29. Richter, H., Grieco, W. J., and Howard, J. B., *Combust. Flame* 119:1–22 (1999).

*Received 24 April 2000; revised 5 December 2000; accepted 20 December 2000*